Thermodynamic Modelling of an Ejector with Compressible Flow by a One-Dimensional Approach

Yveline Marnier Antonio, Christelle Périlhon, Georges Descombes, Claude Chacoux

Entropy **2012**, *14*, 599-613; doi:10.3390/e14040599

OPEN ACCESS

entropy

ISSN 1099-4300

www.mdpi.com/journal/entropy

Article

Thermodynamic Modelling of an Ejector with Compressible Flow by a One-Dimensional Approach

Yveline Marnier Antonio, Christelle Périlhon, Georges Descombes * and Claude Chacoux †

Laboratoire de génie des procédés pour l'environnement, l'énergie et la santé, LGP2ES-EA21, Cnam, case 2D3P20, 292 rue Saint Martin, 75141 Paris cedex 03, France;
E-Mails: yveline.marnier@climespace.fr (Y.M.A.); christelle.perilhon@cnam.fr (C.P.)

† Deceased.

* Author to whom correspondence should be addressed; E-Mail: georges.descombes@cnam.fr; Tel.: +33-1-4027-2000; Fax: +33-1-4271-9329.

Received: 10 January 2012; in revised form: 9 March 2012 / Accepted: 12 March 2012 / Published: 23 March 2012

Abstract: The purpose of this study is the dimensioning of the cylindrical mixing chamber of a compressible fluid ejector used in particular in sugar refineries for degraded vapor re-compression at the calandria exit, during the evaporation phase. The method used, known as the "integral" or "thermodynamic model", is based on the model of the one-dimensional isentropic flow of perfect gases with the addition of a model of losses. Characteristic curves and envelope curves are plotted. The latter are an interesting tool from which the characteristic dimensions of the ejector can be rapidly obtained for preliminary dimensioning (for an initial contact with a customer for example). These ejectors, which were specifically designed for the process rather than selected from a catalog of standard devices, will promote energy saving.

Keywords: thermodynamic model; static compression; ejector; 1D modelling; compressible fluid; design

---

Nomenclature

Symbols

C_p	Specific heat at constant pressure, J/(kg.K)
F_3	Pressure loss coefficient in the diffuser
H	Total enthalpy, J
I	Impulse or dynalpy, J
P	Total pressure, Pa
P_{t3}	Total pressure at mixing chamber exit, Pa
P_{r3}	Total outlet pressure in diffusor exit, Pa
p	Static pressure, Pa
q	Mass flow, kg/s
r	Mayer constant, J/(kg.K)
S_{col}	Throat section of driving flow nozzle, m^2
S_1	Inlet mixing chamber section of driving flow, m^2
S_2	Inlet mixing chamber section of induced flow, m^2
S_3	Section of the cylindrical mixing chamber, m^2
T	Total air temperature, K
t	Static temperature, K
V	Mean velocity of the various flows, m/s

Subscripts

1	primary driving flow at the exit of the driving nozzle, mixing chamber inlet
2	secondary induced flow at the mixing chamber inlet
3	mixed flows at the mixing chamber outlet

Greek Letters

ρ	Density, kg/m^3
γ	Fluid cP/cv ratio

1. Introduction

A jet ejector is a device which uses the kinetic energy of a driving fluid, injected under pressure by a convergent or convergent-divergent nozzle into a zone of lower pressure, to suck in and entrain a secondary fluid with low pressure (of a comparable or different nature) and to compress the mixed flow thus obtained to the desired intermediate pressure [1].

Some specialized companies produce tailor-made devices for the food processing industry (distillation plants, sugar refineries), for the desalination of sea water, and for oil. Manufacturers have more or less detailed catalogs of standard devices. In addition to basic theoretical methods, they possess the requisite know-how and experience to obtain the desired performance.

In this study, we present a method to define the ejectors so as to enhance their adaptation to the process concerned and thus to achieve increased energy saving. The application considered here is the sugar refinery process. We will focus more particularly on compressible fluid ejectors with a cylindrical mixing chamber and we will present their dimensioning by the method known as the integral method.

2. Brief Literature Survey

The literature on ejectors is extensive. Eames [2], for example, proposed a new formulation of the equation of momentum applied to the modeling of a supersonic jet ejector pump. Eames [3] also conducted an experimental and analytical study of a steam ejector refrigeration machine. Fan *et al.* [4] proposed a compressible fluid CFD model of a jet in an ejector pump. Rogdakis and Alexis [5] carried out a 1D analytical study to characterize the performance of an ejector system used for air conditioning, and in a complementary study [6] they investigated an ejector design using a two-phase mixture NH_3-H_2O based on the theory of Keenan *et al.*

A major contribution was made by Gilbert and Hill [7] in their 2D characterization of a variable geometry jet exhaust in terms of pressure and flow velocity distribution. Deberne *et al.* [8] proposed a numerical description of a 1D steam injector comprising a supersonic layer in the jet. Sobieski [9] developed a CFD analysis based on the compressible fluid description of a 2D air flow, but noted that the simulation results were not fully validated by experimental results (due to the lack of appropriate models of turbulence and mixing in the code used).

Finally, the thesis by Watanawanavet [10] mainly concerns a CFD analysis of energy conversion efficiency in an ejector as a function of its geometry. However, the literature remains sparse for the application considered in this article. This broad study is therefore devoted to sugar refineries and based on a craft approach validated by several hundred cases.

3. Context

The integral method used in this study is based on the model of a one-dimensional isentropic flow of perfect gases. It considers the characteristics of the driving and induced fluids at the mixing chamber inlet and the characteristics of the mixture at the mixing chamber exit, while including initial assumptions [11,12].

When ordering an ejector, the customer specifies the total pressures P_1 of the motive fluid and P_2 of the induced fluid, the associated total temperatures T_1, T_2, the entrainment ratio q_2/q_1 (driving flow/induced flow) or the total outlet pressure P_{r3} (Figure 1). The designer defines the Mach number M_2 of the induced flow to obtain the best performance.

For certain applications, the customer requires a given outlet pressure P_{r3}, in which case the designer calculates the entrainment ratio q_2/q_1 or *vice versa*. In this study, we have imposed the entrainment ratio q_2/q_1.

We will therefore have to calculate the outlet pressure P_{r3} to which a model of pressure loss F_3 (related to the design and scale of the device considered) will be attributed by the designer based on his experience.

The calculation of P_{r3} will then enable the dimensions of the mixing chamber to be determined by calculating its section S_3 as well as the other dimensions of the ejector, which are beyond the scope of this study. The calculated section S_3 of the mixing chamber is a function of the ejector operating conditions, in particular of P_1, T_1, P_2, T_2, but also of q_1, q_2 and P_{r3}.

Figure 1. Diagram of the studied ejector specifying the notations at the various points.

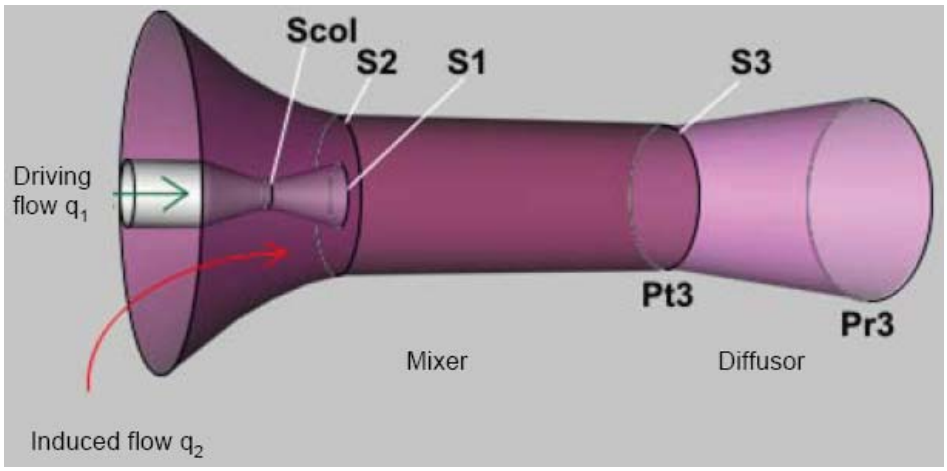

As a concrete example, Figure 2 shows a tailor-made steam-ejector designed for the sugar refinery in Wanze (Belgium) with the following characteristics.

Figure 2. Example of a tailor-made ejector.

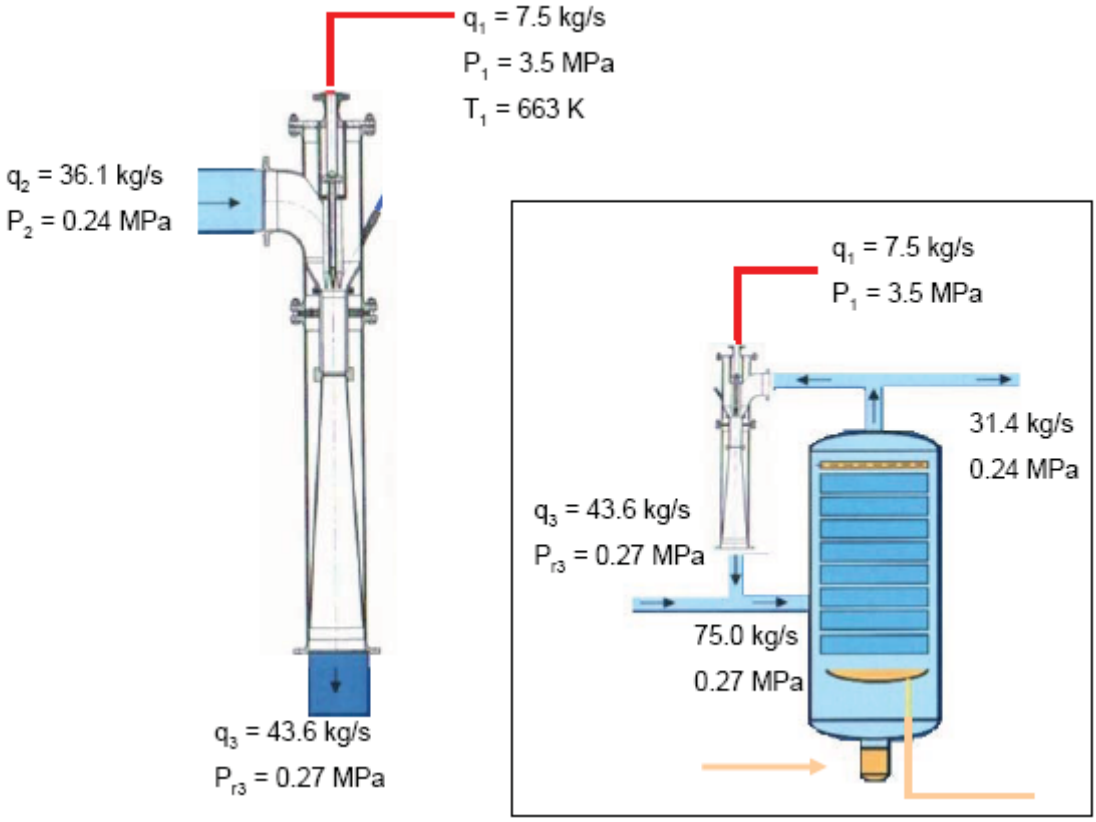

Driving stream

Total pressure: $P_1 = 3.5$ MPa

Total temperature: $T_1 = 663$ K (390°C)

Driving flow: $q_1 = 7.5$ kg/s (27 ton/hour)

Induced stream

Total pressure: $P_2 = 0.24$ MPa

Induced flow: $q_2 = 36.1$ kg/s (130 ton/hour)

Entrainment ratio (driving flow/induced flow): $q_2/q_1 = 4.814$

Mix

Total outlet pressure: $P_{r3} = 0.27$ MPa (absolutes)

These devices are thus adapted to the specific conditions of each company. In sugar refineries, the ejectors are used during the evaporation stage (Figure 3) to increase the pressure level of the vapor mists produced at the exit of the calandrias, thus reducing the energy requirement. It is static compression.

Figure 3. General diagram of an evaporator with use of an ejector.

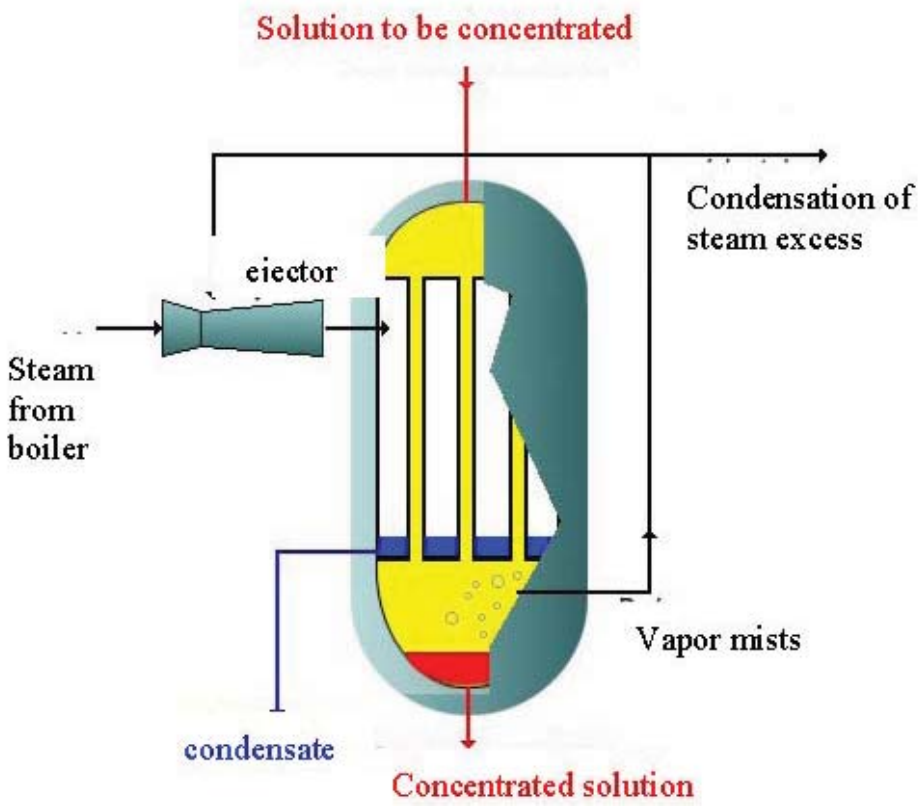

2. Theoretical Thermodynamic Model

The integral calculation method is based on the laws of dynalpy conservation ($I = pS + qV$) in the mixing chamber, of mass and energy conservation between the streams inlet and the mixed flow outlet.

The mixture is assumed to be complete on the outlet side of the mixing chamber and a total pressure loss corresponding to that of the mixing chamber and the diffuser is taken into account. This leads to a

model of pressure loss (F_3) which is dependent on the design and scale of the device considered. This method, which involves implementing Fanno and Rayleigh curves [13], is the most direct but requires experience with various devices to determine the pressure loss model F_3.

2.1. Basic Equations Used

The basic equations used to determine the computation formulae are presented on Figure 4 and are detailed hereafter. They are valid in compressible and incompressible fluids.

Figure 4. Basic equations used.

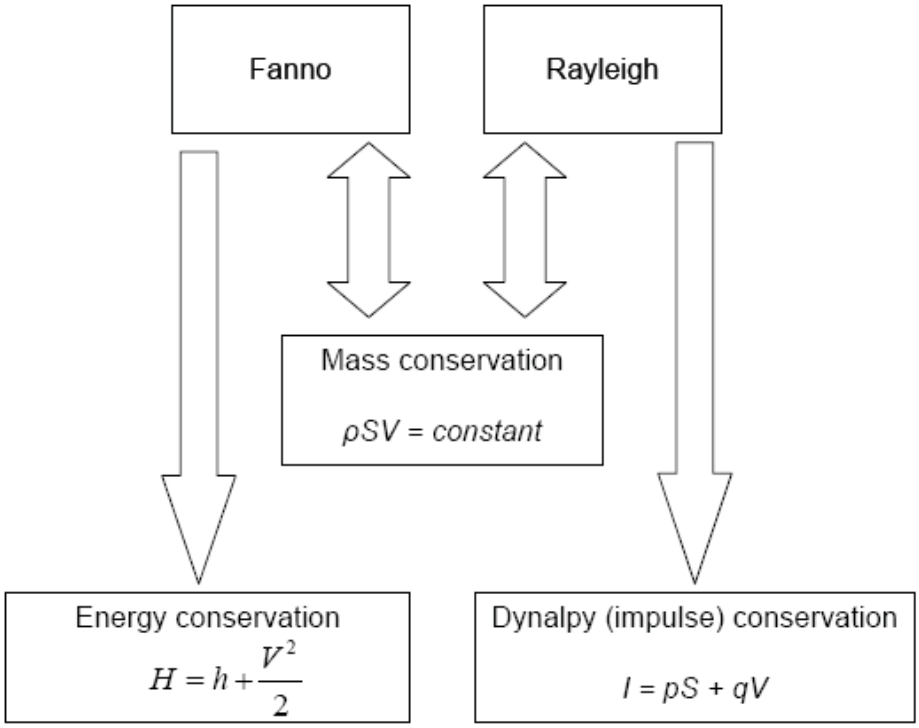

Subscripts 1 and 2 are used respectively for the driving and the induced fluids in the mixing chamber inlet, and subscript 3 for the mixture on the outlet side of the mixing chamber. Total quantities are in capital letters and static quantities in lower case.

2.1.1. Continuity Equation:

$$q_3 = q_1 + q_2 \tag{1}$$

with q = ρSV

2.1.2. Momentum Equation (or dynalpy conservation):

$$p_1S_1 + q_1V_1 + p_2S_2 + q_2V_2 = p_3S_3 + q_3V_3 = I \tag{2}$$

2.1.3. Energy Equation

$$q_1H_1 + q_2H_2 = q_3H_3 \tag{3}$$

The fluids are now assumed to be perfect gases:

$$q_1 c_{p1} T_1 + q_2 c_{p2} T_2 = q_3 c_{p3} T_3 \tag{4}$$

$$q_1\left(c_{p1}t_1 + \frac{V_1^2}{2}\right) + q_2\left(c_{p2}t_2 + \frac{V_2^2}{2}\right) = q_3\left(c_{p3}t_3 + \frac{V_3^2}{2}\right) \tag{5}$$

2.2. Calculation Assumptions

The fluids behave as perfect gases. However the driving can take place only for viscous fluids. The flow is one-dimensional and isentropic to initialize the calculation. It is then supplemented by a model of pressure loss based on experience. The model of pressure loss is deduced from the following relation where P_{t3} is the total pressure at the mixing chamber exit. P_{r3} is the total pressure at the diffuser exit:

$$P_{r3} = P_{t3} - F_3\left(P_{t3} - p_3\right) \tag{6}$$

At the mixing chamber inlet, the static pressures p_1 and p_2 are equal. The mixture is complete at the mixing chamber outlet [2].

From the parameters fixed by the customer, *i.e.*, pressure, flow and temperature, P_1, q_1, T_1, for the driving fluid and P_2, q_2, T_2, for the induced fluid, as well as a loss ratio F_3 fixed by the designer (constant value for a given ejector), we established computation formulae so as to obtain the following parameters in this order:

t_2, p_2, V_2, ρ_2, S_2 for the induced fluid

T_1, ρ_1, V_1, S_1 for the driving fluid

S_3, T_3, V_3, T_3, ρ_3, P_{t3}, P_{r3} for the mixture.

All these formulae were computed then a validation of the computed code was conducted using the steam ejector described below.

2.3. Validation of the Computer Code

Measurements were carried out on a 12 ton/hour driving flow device, commissioned in the marketing year 2005/2006 (sugar refinery in Roye, France). This device had been defined for the following operating conditions (Table 1):

Table 1. Operating conditions defined for a 12 ton/hour device.

P_1 (MPa)	T_1 (K)	P_2 (MPa)	T_2 (K)	q_2/q_1
4.1	673	0.27	402.5	**3.62**

Based on the long-standing experience of the designer and co-author (C. Chacoux), F_3 was imposed [see Equation (6)] and the Mach number chosen for the induced fluid was $M_2 = 0.75$ (the choice of this value is reconsidered below).

2.3.1. Results of Calculations (Table 2)

Table 2. Results of calculation.

P_{r3} (MPa)	T_3 (K)	H_1 (kJ/kg)	H_2 (kJ/kg)	H_3 (kJ/kg)	S_3 (cm^2)
0.34	**454.8**	3 154	2 719	2 809	322

2.3.2. Results of Measurements

The total outlet pressure P_{r3} finally obtained was 0.32 MPa for 0.34 calculated, the observed entrainment ratio q_2/q_1 being slightly different from that proposed (Table 3).

Table 3. Results of measurements for $S_3 = 322$ cm^2.

P_1 (MPa)	T_1 (K)	P_2 (MPa)	T_2 (K)	q_2/q_1
4.5	675.5	0.254	401	**3.58**
P_{r3} (MPa)	**T_3 (K)**	**H_1 (kJ/kg)**	**H_2 (kJ/kg)**	**H_3 (kJ/kg)**
0.31/0.32	**454.5**	3 213	2 717	2 825

Calculation predicted a backpressure of $P_{r3} - P_2 = 0.34 - 0.267 = 0.073$ MPa, whereas experimentation gave $P_{r3} - P_2 = 0.32 - 0.254 = 0.066$ MPa. This slight difference can be explained by the fact that P_2 is a little different in the two cases (2.67 MPa calculated, 2.54 MPa measured, *i.e.*, a discrepancy of 0.5%). Similarly, the driving pressure was 4.5 MPa instead of 4.1 previously considered during the design process, resulting in a drop in the driving rate. All these results are coherent and satisfactory.

3. Use of the Ejector in Conditions Different from the Nominal Point

The ejector is determined for a nominal operating point. However, the process conditions may change, in which case the user must be able to determine new values of the parameters (for instance the new driving flow for the same induced flow).

For this purpose, characteristic curves may be of assistance. If the range of operation is too wide, several ejectors must be considered in order to operate with optimum efficiency. To achieve this, an extension of the computed code is possible by imposing the ratio of the mixing chamber section to the throat section of the driving flow nozzle S_3/S_{col} as the reference criterion.

For S_{col} fixed, depending on the S_3 section—called the origin section herein—The induced flow q_2 is adjusted (for various values of the Mach number M_2) until $S_{3\,calcul} \approx S_{3\,origin}$ is obtained.

Using the various values of the induced flow q_2, the various values of the outlet pressure P_{r3} are calculated and the backpressure ($P_{r3} - P_2$) is plotted against the driving rate q_2/q_1, the driving flow q_1 and the induced flow total pressure P_2 being fixed.

3.1. Plotting a Characteristic Curve

Figure 5 plots the characteristic curve of a given geometry (S_3/S_{col}) related to the primary and secondary characteristics of the above steam ejector (q_1 fixed).

Figure 5. Characteristic curve of the ejector (q_1 fixed).

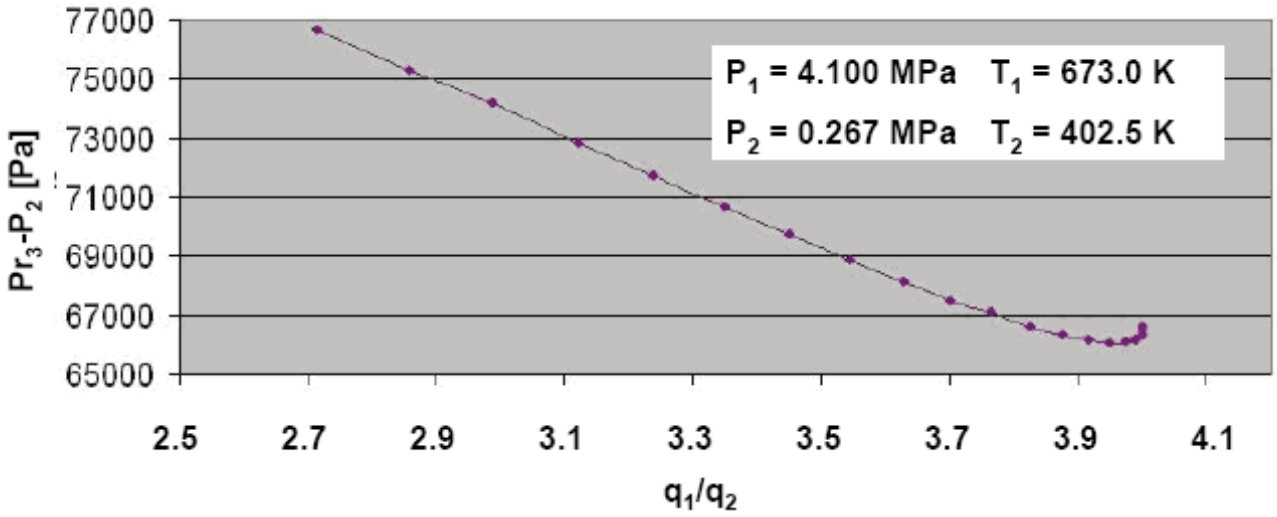

Note that the bent part of the curve on the right of the graph is not a true representation because of the transonic effects in this zone. With such a curve, if the discharge pressure imposed by the process changes, the user will be able to determine the new driving flow q_1 required for the same induced flow q_2.

In addition, as mentioned above, for each point on this curve there is a corresponding Mach number M_2. The efficiency calculation at each point shows that the Mach number is maximum at the minimum point of the curve (see Section 4.1).

3.2. Plotting Several Characteristic Curves

The farther from the nominal (or design point or point of greatest efficiency) the point is, the more the ejector efficiency drops. Thus it is not interesting to widen the operating range too much. It is preferable to consider another ejector when the conditions $P_{r3} - P_2$ or q_2/q_1 differ considerably. If the installation undergoes strong variations, several ejectors can be laid out in parallel, gauged for suitable flow ranges. A series of characteristic curves is thus constructed.

4. Envelope Curves: Geometry Definition for Optimum Efficiency

To quickly obtain the initial elements of a dimensioning for the first contact with a customer, it is advisable to know the envelope curves of a family of devices. Given a geometry S_3/S_{col} and the driving, induced and outlet pressure and temperature conditions, these curves can then be used to define the most efficient geometry of the device(s).

4.1. Definition of an Envelope Curve

The envelope curve is a curve (C) defined by a whole set of curves (C_i), such that each curve is tangent in at least one point of (C) and that in any point of (C), a curve (C_i) tangent with (C) exists. In fact in our study, curves (C_i) are the characteristic curves.

The points of tangency of the envelope curves with the characteristic curves are the points of the characteristic curves located at the level of the minimum point. These points are the optimal operating points of the ejectors, *i.e.*, where the total efficiency is maximum.

The total effectiveness of an ejector results in the total efficiency which can be defined by the ratio between the compression energy recovered on total flow and the energy spent on the driving flow expansion in the nozzle. Its expression is:

$$\eta_g = \frac{q_3(\gamma_1 - 1)T_3\gamma_3 r_3\left[1-\left(\frac{P_2}{P_3}\right)^{\frac{\gamma_3-1}{\gamma_3}}\right]}{q_1(\gamma_3 - 1)T_1\gamma_1 r_1\left[1-\left(\frac{P_2}{P_1}\right)^{\frac{\gamma_1-1}{\gamma_1}}\right]} \quad (7)$$

Optimum Example of Operating Point on the Characteristic Curves

From the X-coordinates q_2/q_1, we calculated the ordinates $P_{r3} - P_2$ of certain points around the minimum point of the characteristic curve presented on Figure 5. We also calculated the corresponding total efficiency η_g for each point and drew up Table 4.

Table 4. Ejector global efficiency.

q_2/q_1	M_2	$P_{r3} - P_2$ (Pa)	η_g (%)
2.715	0.43	76 662	34.41
2.988	0.49	74 198	35.62
3.239	0.55	71 738	36.58
3.875	0.79	66 313	38.72
3.949	**0.85**	**66 069**	**44.22**
3.974	0.88	66 086	39.15
3.991	0.91	66 162	39.25
4.000	0.94	66 325	39.21

It can be seen that this minimum point is the point of the coordinates $q_2/q_1 = 3.949$ and $P_{r3} - P_2 = 66\,069$ Pa which corresponds to the best performance $\eta_g = 0.4422$.

The calculation of the following points corresponding to higher driving rates is no longer valid because of the transonic effects not taken into account by this calculation: the losses in the diffuser can no longer be regarded as constant.

Figure 6 shows an expanded view of the characteristic curve plotted on Figure 5. The minimum point of the characteristic curve is indicated by an arrow.

Figure 6. Expanded view of the characteristic curve, showing the point of maximum efficiency (q_1 and S_3 fixed).

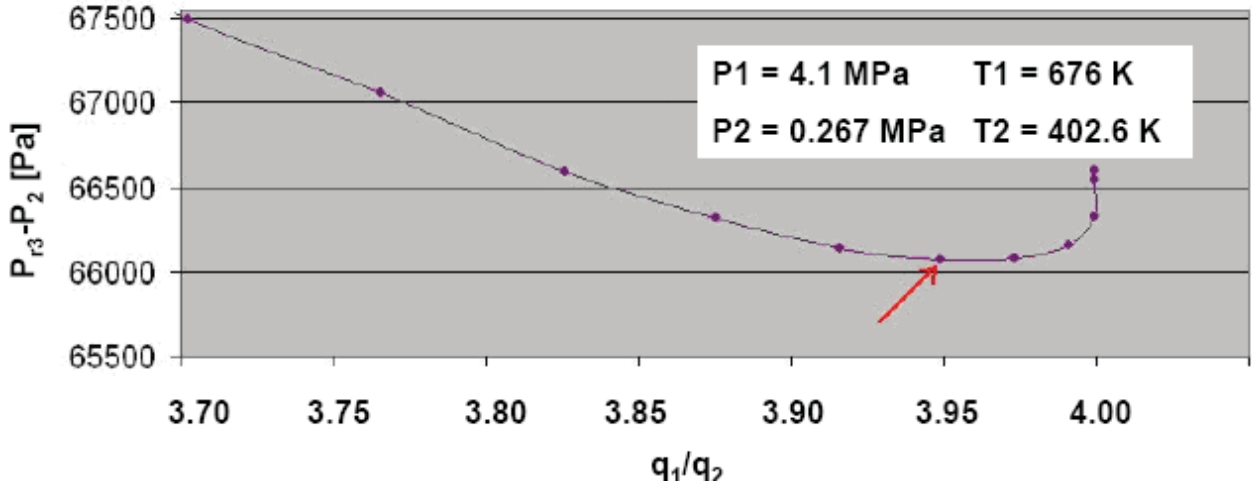

From the whole set of these optimum operating points (from each curve on Figure 7) the envelope curve valid for a single value of the total driving pressure P_1 and total driving temperature T_1 can be plotted.

Figure 7. Characteristic curves of ejectors of various sections (q_1 fixed).

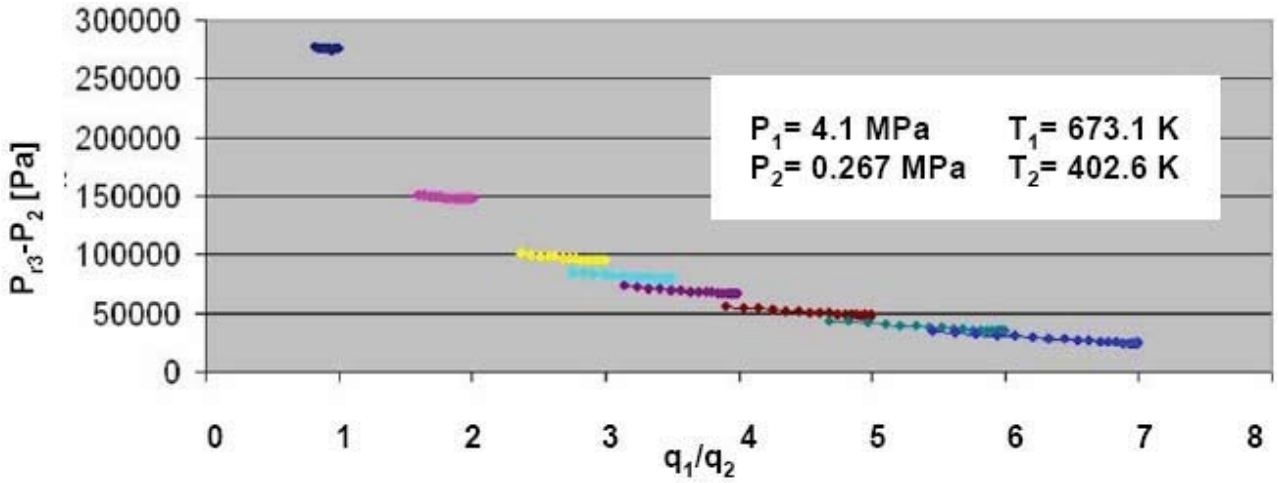

When the values of P_1 and T_1 are modified, the other parameters P_2, T_2 and q_1 remaining unchanged, a new envelope curve is obtained (Figure 8).

Figure 8. Envelope curves for various values of P_1 and T_1 (q_1 fixed).

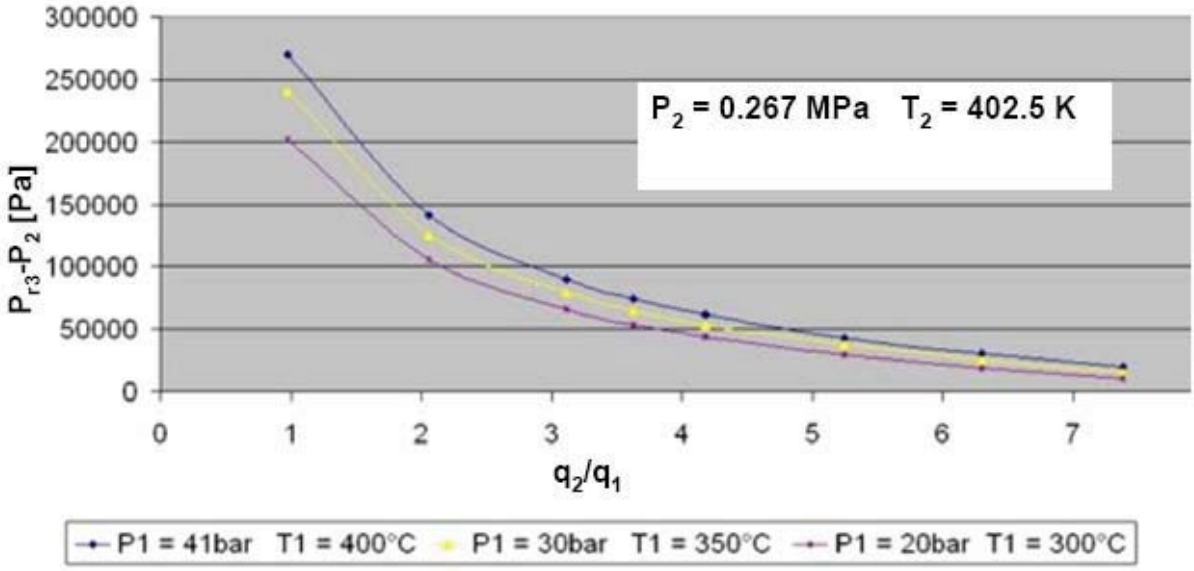

4.2. Validation of the Envelope Curve

The previous example (Section 2.3) of an ejector defined for the following conditions is again taken (Table 5).

Table 5. Operating conditions defined for a 12 ton/hour device.

P_1 (MPa)	T_1 (K)	P_2 (MPa)	T_2 (K)	q_2/q_1
4.1	673	0.267	402.5	**3.62**

The matching envelope curve is the curve of characteristics P_1 = 4.1 MPa and T_1 = 673K (400 °C). For q_2/q_1 = 3.62 the following values can be read off the graph: $P_{r3} - P_2$ = 73 600 Pa, P_2 = 0.267 MPa, which gives P_{r3} = 0.3406 MPa. This point can be seen on Figure 9.

Figure 9. Envelope curves (q_1 fixed).

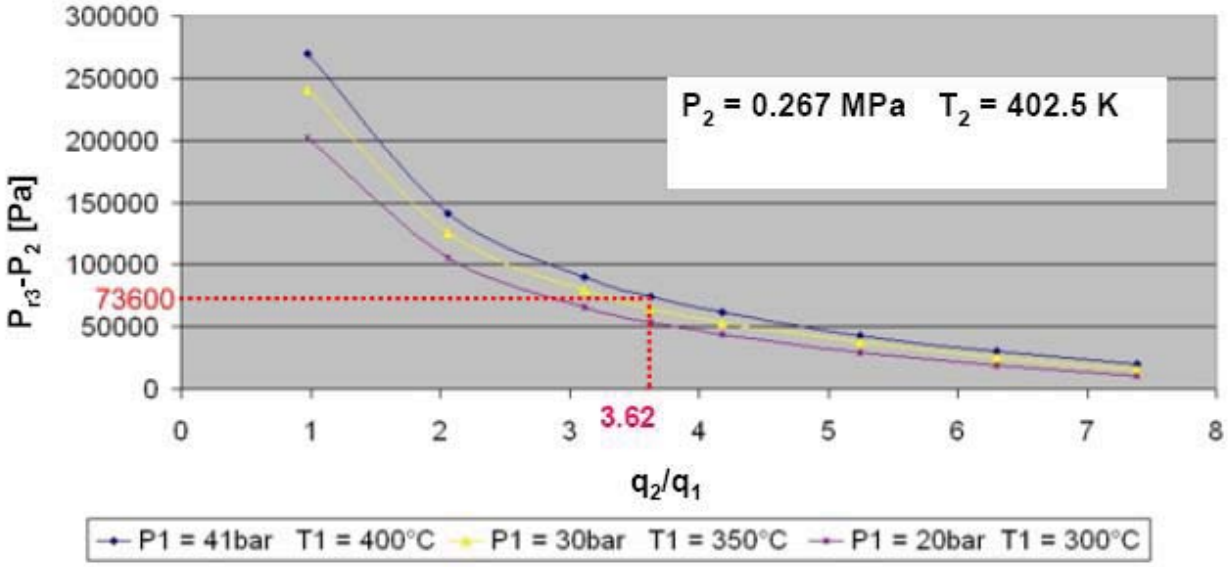

We recap below the results of measurements (Table 6).

Table 6. Results of measurement for a 12 ton/hour device.

P_1 (MPa)	T_1 (K)	P_2 (MPa)	T_2 (K)	P_3 (MPa)
4.5	675.5	0.254	401	0.32

In light of these results, it can be considered that the use of the envelope curve during an initial customer contact provides a very good idea of the device to be dimensioned. These envelope curves depend, however, on many parameters. For other values of total pressure and temperature of the induced fluid P_2 and T_2, as well as the driving fluid flow q_1, it will therefore be necessary to have new envelope curves. Likewise, it will be necessary to interpolate between these curves for values of P_1 and T_1 that are different from those plotted.

The situation is greatly improved by using reduced co-ordinates which allows the aggregation of these various curves into a single one (but always given P_2, T_2 and q_1) as shown on the following example of Figure 10:

$$\frac{P_{r3}^{\frac{\gamma_3-1}{\gamma_3}} - P_2^{\frac{\gamma_2-1}{\gamma_2}}}{P_1^{\frac{\gamma_1-1}{\gamma_1}} - P_{r3}^{\frac{\gamma_3-1}{\gamma_3}}} \cdot \left(\frac{P_1^{\frac{\gamma_1-1}{\gamma_1}}}{P_2^{\frac{\gamma_2-1}{\gamma_2}}} \right) = f\left(\frac{q_2}{q_1}\sqrt{\frac{r_2 T_2 \gamma_1}{r_1 T_1 \gamma_2}}\right) \tag{8}$$

Figure 10. Condensed envelope curve (for T_2, P_2, q_1 fixed).

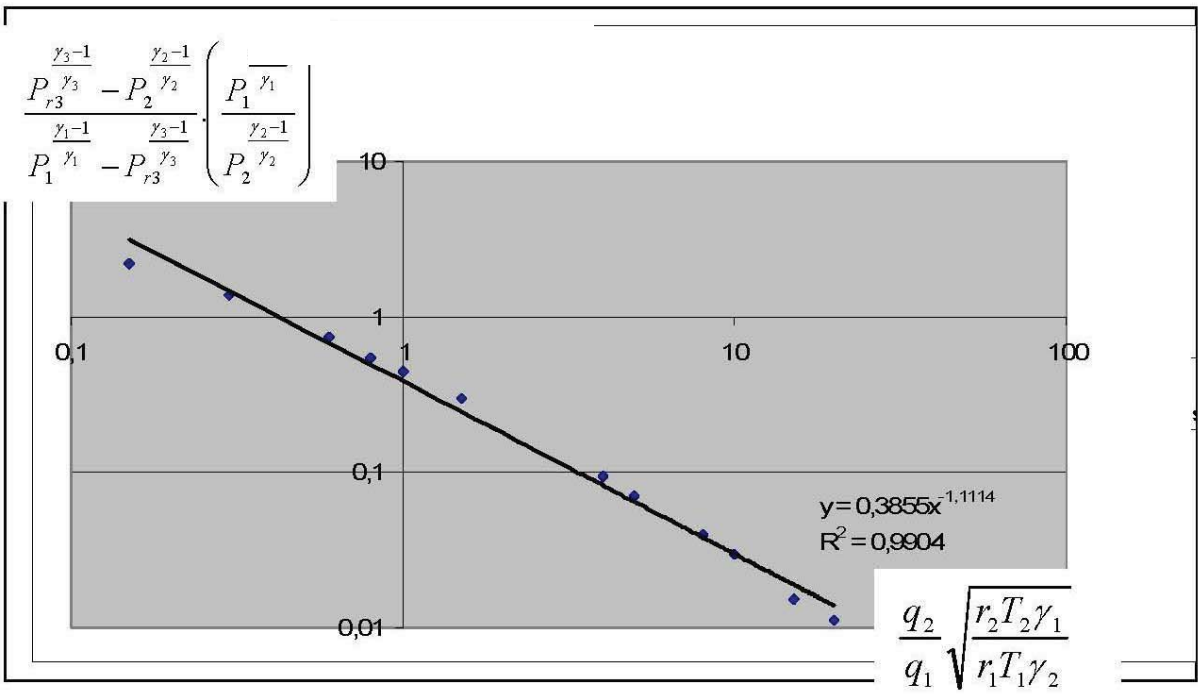

5. Conclusions

This paper has presented:

1. A study of the dimensioning of compressible fluid ejectors with a cylindrical mixing chamber, used, amongst other applications, in sugar refineries during the evaporation stage. The computed code, worked out thanks to the integral method, was validated on more than three hundred steam ejectors with a discrepancy between calculation and measurements of less than 5%.
2. The thermodynamic model used is based on the model of the one-dimensional isentropic flow of perfect gases with the addition of a model of losses. It helps to make appropriate technological choices when designing new installations or during the rehabilitation of existing ones, by favouring energy economy.
3. This method could be exploited for the dimensioning of compressible fluid ejectors with a conical mixing chamber. The study would however be more complex because the driving of secondary flow in this type of mixing chamber is supersonic.

Acknowledgements

In memory of our colleague and co-author, Claude Chacoux.

References

1. Paulon, J. Ejecteurs (in French). *Techniques de l'ingénieur* **1993**, B4250. Available online: http://www.techniques-ingenieur.fr (accessed on 19 March 2012).
2. Eames, I.W. A new prescription for the design of supersonic jet-pumps: The constant rate momentum change method. *Appl. Therm. Eng.* **2002**, *22*, 121–131.
3. Eames, I.W.; Aphornratana, S.; Haider H. A theoretical and experimental study of a small-scale steam jet refrigerator. *Int. J. Refrig.* **1995**, *18*, 378–386.
4. Fan, J.; Eves, J.; Thompson, H.M.; Toropov, V.V.; Kapur, N.; Copley, D.; Mincher, A. Computational fluid dynamic analysis and design optimisation of jet pumps. *Comput. Fluid.* **2001**, *46*, 212–217.
5. Rogdakis, E.D.; Alexis, G.K. Design and parametric investigation of an ejector in an air-conditioning system. *Appl. Therm. Eng.* **2000**, *20*, 213–226.
6. Rogdakis, E.D.; Alexis, G.K. Investigation of ejector design at optimum operating condition. *Energ. Convers. Manag.* **2000**, *41*, 1841–1849.
7. Gilbert, G.B.; Hill, P.G. Analysis and testing of two-dimensional slot nozzle ejectors with variablearea mixing sections; NASA contractor report CR-2251; NASA: Washington, DC, USA, May 1973.
8. Deberne, N.; Leone, J.F.; Duque, A.; Lallemand, A. A model for calculation of steam injector performance. *Int. J. Multiphas. Flow.* **1999**, *25*, 841–855.
9. Sobieski, W. Performance of an air-air ejector: An attempt at numerical modelling. *Task Quarterly* **2003**, *7*, 449–457.
10. Watanawanavet, S. Optimization of a high-efficiency jet ejector by computational fluid dynamics software. Master Thesis, Texas A&M University: College Station, TX, USA, May 2005.

11. Chacoux, C. *Définition et fonctionnement des stato-surpresseurs et des stato-compresseurs*; BERTIN: Paris, France, 1980.
12. Marnier, Y. Dimensionnement d'un mélangeur à jet en écoulement compressible monodimensionnel. Master Thesis. Cnam: Paris, France, 2006.
13. Hansen, A. *Fluid Mechanics*; WILEY: New York, NY, USA, 1967.